Microbial decomposition processes and vulnerable Arctic soil organic carbon in the 21st century

Junrong Zha and Qianlai Zhuang

Department of Earth, Atmospheric, and Planetary Sciences and Department of Agronomy, Purdue University, West Lafayette, IN 47907 USA

Submitted to: *Biogeoscience*

Correspondence to: qzhuang@purdue.edu

Abstract

Inadequate representation of biogeochemical processes in current biogeochemistry models contributes to a large uncertainty in carbon budget quantification. Here, detailed microbial mechanisms were incorporated into a process-based biogeochemistry model, the Terrestrial Ecosystem Model (TEM). Ensemble regional simulations with the new model (MIC-TEM) estimated the carbon budget of the Arctic ecosystems is 76.0±114.8 Pg C during the 20th century, -3.1±61.7 Pg C under the RCP 2.6 scenario and 94.7±46 Pg C under the RCP 8.5 scenario during the 21st century. Positive values indicate the regional carbon sink while negative values are source to the atmosphere. Compared to the estimates using a simpler soil decomposition algorithm in TEM, the new model estimated that the Arctic terrestrial ecosystems stored 12 Pg less carbon over the 20th century, 19 Pg C and 30 Pg C less under the RCP 8.5 and RCP 2.6 scenarios, respectively, during the 21st century. When soil carbon within depths 30 cm, 100 cm and 300 cm was considered as initial carbon in the 21st century simulations, the region was estimated to accumulate 65.4, 88.6, and 109.8 Pg C, respectively, under the RCP 8.5 scenario. In contrast, under the RCP 2.6 scenario, the region lost 0.7, 2.2, and 3 Pg C, respectively, to the atmosphere. We conclude that the future regional carbon budget evaluation largely depends on whether or not the adequate microbial activities are represented in earth system models and the sizes of soil carbon considered in model simulations.

1. Introduction

Northern high-latitude soils and permafrost contain more than 1,600 Pg carbon (Tarnocai et al., 2009). Climate over this region has warmed in recent decades (Serreze and Francis, 2006) and the increase is 1.5 to 4.5 times the global mean (Holland and Bitz, 2003). Warming-induced changes in carbon cycling are expected to exert large feedbacks to the global climate system (Davidson and Janssens, 2006; Christensen and Christensen, 2007; Oechel et al., 2000).

Warming is expected to accelerate soil C loss by increasing soil respiration, but increasing nutrient mineralization, thereby stimulating plant net primary production (NPP) (Mack et al., 2004). Thus, the variation of climate may switch the role of the Arctic system between a C sink and a source if soil C loss overtakes NPP (Davidson et al., 2000; Jobbágy and Jackson, 2000). Process-based biogeochemical models such as TEM (Hayes et al., 2014; Raich and Schlesinger, 1992; McGuire et al., 1992; Zhuang et al., 2001, 2002, 2003, 2010, 2013), Biome-BGC (Running and Coughlan, 1988), CASA (Potter et al., 1993), CENTURY (Parton et al., 1994) and Biosphere Energy Transfer Hydrology scheme (BETHY) (Knorr et al., 2000) have been widely used to quantify the response of carbon dynamics to climatic changes (Todd-Brown et al., 2012). An ensemble of process-based model simulations suggests that arctic ecosystems acted as a sink of atmospheric CO_2 in recent decades (McGuire et al., 2012; Schimel et al., 2013). However, the response of this sink to increasing levels of atmospheric CO_2 and climate change is still uncertain (Todd-Brown et al., 2013). The IPCC 5th report also shows that land carbon storage is the largest source of uncertainty in the global carbon budget quantification (Ciais et al., 2013).

Much of the uncertainty is also due to the inadequate representation of ecosystem processes that determine the exchanges of water, energy and C between land ecosystems and the atmosphere (Wieder et al., 2013), and ignorance of some key biogeochemical mechanisms (Schmidt et al., 2011). For example, heterotrophic respiration (R_H) is the primary loss pathway for soil organic carbon (Hanson et al., 2000; Bond-Lamberty and Thomson, 2010), and it generally increases with increasing temperature (Davidson and Janssens, 2006) and moisture levels in well-drained soils (Cook and Orchard, 2008). Moreover, this process is closely related to soil nitrogen mineralization that determines soil N availability and affects gross primary production (Hao et al., 2015). To date, most models treated soil decomposition as a first-order decay process, i.e., CO_2 respiration is directly proportional to soil organic carbon. However, it is not clear if these models are robust under changing environmental conditions (Lawrence et al., 2011; Schimel and Weintraub, 2003; Barichivich et al., 2013) since they often ignored the effects of changes in biomass and composition of decomposers, while recent empirical studies have shown that microbial abundance and community play a significant role in soil carbon decomposition (Allison and Martiny, 2008). The control that microbial activity and enzymatic kinetics imposed on soil respiration suggests the need for explicit representation of microbial physiology, enzymatic activity, in addition to the direct effects of soil temperature and soil moisture on heterotrophic respiration (Schimel and Weintraub, 2003). Recent mechanistically-based models explicitly incorporated with the microbial dynamics and enzyme kinetics that catalyze soil C decomposition have produced notably different results and a closer match to contemporary observations (Wieder et al., 2013; Allison et al., 2010) indicating the need for

89 incorporating these microbial mechanisms into large-scale earth system models to quantify
90 carbon dynamics under future climatic conditions ((Wieder et al., 2013; Allison et al., 2010).
91 This study advanced a microbe-based biogeochemistry model (MIC-TEM) based on an
92 extant Terrestrial Ecosystem Model (TEM) (Raich and Schlesinger, 1992; McGuire et al., 1992;
93 Zhuang et al., 2001, 2002, 2003, 2010, 2013; Hao et al., 2015). In MIC-TEM, the heterotrophic
94 respiration is not only a function of soil temperature, soil organic matter (SOM) and soil
95 moisture, but also considers the effects of dynamics of microbial biomass and enzyme kinetics
96 (Allison et al., 2010). The verified MIC-TEM was used to quantify the regional carbon dynamics
97 in northern high latitudes (north 45 °N) during the 20th and 21st centuries.
98
99 **2. Methods**
100 **2.1 Overview**
101 Below we first briefly describe how we advanced the MIC-TEM by modifying the soil
102 respiration process in TEM (Zhuang et al., 2003) to better represent carbon dynamics in
103 terrestrial ecosystems. Second, we describe how we parameterized and verified the new model
104 using observed net ecosystem exchange data at representative sites and how simulated net
105 primary productivity (NPP) was evaluated with Moderate Resolution Imaging Spectroradiometer
106 (MODIS) data to demonstrate the reliability of new model at regional scales. Third, we present
107 how we applied the model to the northern high latitudes for the 20th and 21st centuries. Finally,
108 we introduce how we conducted the sensitivity analysis on initial soil carbon input, using
109 gridded observation-based soil carbon data of three soil depths during the 21st century.
110

2.2 Model description

TEM is a highly aggregated large-scale biogeochemical model that estimates the dynamics of carbon and nitrogen fluxes and pool sizes of plants and soils using spatially referenced information on climate, elevation, soils and vegetation (Raich and Schlesinger, 1992; McGuire et al., 1992; Zhuang et al., 2003, 2010; Melillo et al., 1993). To explicitly consider the effects of microbial dynamics and enzyme kinetics on large-scale carbon dynamics of northern terrestrial ecosystems, we developed MIC-TEM by coupling version 5.0 of TEM (Zhuang et al., 2003, 2010) with a microbial-enzyme module (Hao et al., 2015; Allison et al., 2010). Our modification of the TEM improved the representation of the heterotrophic respiration (R_H) from a first-order structure to a more detailed structure (Fig. S1).

In TEM, heterotrophic respiration R_H is calculated as a function of soil organic carbon (SOC), soil temperature (Q_{10}), soil moisture (f (MOIST)), and the gram-specific decomposition constant K_d:

$$R_H = K_d * SOC * Q_{10}^{\frac{DT}{10}} * f(MOIST) \quad (1)$$

where DT is soil temperature at top 20 cm. CO_2 production from SOC pool is directly proportional to the pool size, and the activity of decomposers only depends on the built-in relationships with soil temperature and moisture (Todd-Brown et al., 2012). Therefore, the changes in microbial community composition or adaption of microbial physiology to new conditions were not represented in TEM. However, current studies indicate that soil C decomposition depends on the activity of biological communities dominated by microbes (Schimel and Weintraub, 2003), implying that the biomass and composition of the decomposer community can't be ignored (Todd-Brown et al., 2012).

We thus revised the first-order soil C structure in TEM to a second-order structure considering microbial dynamics and enzyme kinetics according to Allison et al. (2010). In MIC-TEM, heterotrophic respiration (R_H) is calculated as:

$$R_H = ASSIM*(1-CUE) \quad (2)$$

Where ASSIM and CUE represent microbial assimilation and carbon use efficiency, respectively. ASSIM is modeled with a Michaelis-Menten function:

$$ASSIM = Vmax_{uptake}*MIC * \frac{DOC}{Km_{uptake}+DOC} \quad (3)$$

Where DOC is dissolved organic carbon and $Vmax_{uptake}$ is the maximum velocity of the reaction and calculated using the Arrhenius equation:

$$Vmax_{uptake} = Vmax_{uptake_0} * e^{-\frac{Ea_{uptake}}{R*(temp+273)}} \quad (4)$$

$Vmax_{uptake_0}$ is the pre-exponential coefficient, Ea_{uptake} is the activation energy for the reaction ($Jmol^{-1}$), R is the gas constant (8.314 $Jmol^{-1}K^{-1}$), and temp is the temperature in Celsius under the reaction occurs.

Besides, Km_{uptake} value is calculated as a linear function of temperature:

$$Km_{uptake} = Km_{uptake_{slope}} * temp + Km_{uptake_0} \quad (5)$$

Microbial biomass MIC is modeled as:

$$\frac{dMIC}{dt} = ASSIM * CUE - DEATH - EPROD \quad (6)$$

Where microbial biomass death (DEATH) and enzyme production (EPROD) are modeled as proportional to microbial biomass with constant rates r_{death} and $r_{EnzProd}$:

$$DEATH = r_{death}*MIC \quad (7)$$

$$EPROD = r_{EnzProd}*MIC \quad (8)$$

Where r_{death} and $r_{EnzProd}$ are the ratio of microbial death and enzyme production, respectively.

DOC is part of soil organic carbon:

$$\frac{\mathrm{dDOC}}{\mathrm{dt}} = \mathrm{DEATH} * (1 - \mathrm{MICtoSOC}) + \mathrm{DECAY} + \mathrm{ELOSS} - \mathrm{ASSIM} \quad (9)$$

where MICtoSOC is carbon input ratio as dead microbial biomass to SOC, representing the fraction of microbial death that flows into SOC, and is set as a constant value according to Allison et al. (2010). SOC dynamics are modeled:

$$\frac{\mathrm{dSOC}}{\mathrm{dt}} = \mathrm{Litterfall} + \mathrm{DEATH} * \mathrm{MICtoSOC} - \mathrm{DECAY} \quad (10)$$

Where Litterfall is estimated as a function of vegetation carbon (Zhuang et al., 2010). The enzymatic decay of SOC is calculated as:

$$\mathrm{DECAY} = \mathrm{V_{max}}*\mathrm{ENZ} * \frac{\mathrm{SOC}}{Km+\mathrm{SOC}} \quad (11)$$

Where V_{max} is the maximum velocity of the reaction and calculated using the Arrhenius equation:

$$V_{max} = \mathrm{Vmax_0}*\mathrm{e}^{-\frac{Ea}{\mathrm{R}*(\mathrm{temp}+273)}} \quad (12)$$

The parameters Km and carbon use efficiency (CUE) are temperature sensitive, and calculated as a linear function of temperature between 0 and 50°C:

$$Km = \mathrm{Km}_{slope}*\mathrm{temp} + \mathrm{Km_0} \quad (13)$$

$$\mathrm{CUE} = \mathrm{CUE_{slope}}*\mathrm{temp} + \mathrm{CUE_0} \quad (14)$$

Where CUEslope and CUE_0 are parameters for calculating CUE, and Km_{slope} and Km_0 are parameters for calculating Km. The values of $\mathrm{CUE_{slope}}$, $\mathrm{CUE_0}$, Km_{slope}, and Km_0were derived from Allison et al. (2010).

ELOSS is also a first-order process, representing the loss of enzyme:

$$\mathrm{ELOSS} = \mathrm{r_{enzloss}}*\mathrm{ENZ} \quad (15)$$

Where $r_{enzloss}$ is the ratio of enzyme loss. Enzyme pool (ENZ) is modeled:

$$\frac{dENZ}{dt}=EPROD-ELOSS \quad (16)$$

Heterotrophic respiration (R_H) is an indispensable component of soil respiration (Bond-Lamberty and Thomson, 2010), and closely coupled with soil nitrogen (N) mineralization that determines soil N availability, affecting gross primary production (GPP).

2.3 Model parameterization and validation

The variables and parameters of these microbial dynamics and their impacts on soil C decomposition were detailed in Allison et al. (2010) (Table 1). Here we parameterized MIC-TEM for representative ecosystem types in northern high latitudes based on monthly net ecosystem productivity (NEP, gCm^{-2} mon^{-1}) measurements from AmeriFlux network (Davidson et al., 2000) (Table S1). The results for model parameterization was presented in Fig. S2. Another set of level 4 gap-filled NEP data was used for model validation at site level (Table S2). The site-level monthly climate data of air temperature (°C), precipitation (mm) and cloudiness (%) were used to drive the model. Gridded MODIS NPP data from 2001 to 2010 were used to evaluate regional NPP simulation. The MODIS NPP data was developed by the MOD17 MODIS project. The product name is Net Primary Production Yearly L4 Global 1 km. The critical parameter used in MOD17 algorithm is conversion efficiency parameter Ɛ. More information about the MODIS NPP product can be found at https://neo.sci.gsfc.nasa.gov/view.php?datasetId=MOD17A2_M_PSN.

In TEM, NPP is calculated as:

$$NPP=GPP-R_A \quad (17)$$

Where GPP is gross primary production, and R_A is autotrophic respiration.

$$GPP=C_{max}*f(PAR)*f(moist)*f(foliage)*f(T)*f(CO_2)*f(NA) \quad (18)$$

For detailed GPP and R_A calculations, see Zhuang et al. (2003). The parameterization was conducted with a global optimization algorithm SCE-UA (Shuffled complex evolution) (Duan et al., 1994) to minimize the difference between the monthly simulated and measured NEE at these sites (Fig. S2). The cost function of the minimization is:

$$Obj = \sum_{i=1}^{k}(NEP_{obs,i}\text{-}NEP_{sim,i})^2 \quad (19)$$

Where $NEP_{obs,i}$ and $NEP_{sim,i}$ are the observed and simulated NEP, respectively. k is the number of data pairs for comparison. Other parameters used in MIC-TEM were default values from TEM 5.0 (Zhuang et al., 2003, 2010). The optimized parameters were used for model validation and regional extrapolations.

2.4 Regional simulations

Two sets of regional simulations for the 20th century using MIC-TEM and TEM at a spatial resolution of 0.5° latitude × 0.5° longitude were conducted. Gridded forcing data of monthly air temperature, precipitation, and cloudiness were used, along with other ancillary inputs including historical atmospheric CO_2 concentrations, soil texture, elevation, and potential natural vegetation. Climatic inputs vary over time and space, whereas soil texture, elevation, and land cover data are assumed to remain unchanged throughout the 20th century, which only vary spatially. The transient climate data during the 20th century was organized from the Climatic

Research Unit (CRU TS3.1) from the University of East Anglia (Harris et al., 2014). The spatial-explicit data include potential natural vegetation (Melillo et al., 1993), soil texture (Zhuang et al., 2003) and elevation (Zhuang et al., 2015).

Similarly, two sets of simulations were conducted driven with two contrasting climate change scenarios (RCP 2.6 and RCP 8.5) over the 21st century. The future climate change scenarios were derived from the HadGEM2-ES model, which is a member of CMIP5 project (https://esgf-node.llnl.gov/search/cmip5/). The future atmospheric CO_2 concentrations and climate forcing from each of the two climate change scenarios were used. The simulated NPP, R_H and NEP by both models (TEM 5.0 and MIC-TEM) were analyzed. The positive NEP represents a CO_2 sink from the atmosphere to terrestrial ecosystems, while a negative value represents a source of CO_2 from terrestrial ecosystems to the atmosphere.

Besides, in order to test the parameter uncertainty in our model, we conducted the regional simulations with 50 sets of parameters for both historical and future studies. The 50 sets of parameters were obtained according to the method in Tang and Zhuang (2008). The upper and lower bounds of the regional estimations were generated based on these simulations.

2.5 Sensitivity to initial soil carbon input

Future carbon dynamics can be affected by varying initial soil carbon amount. In the standard simulation of TEM, the initial soil carbon amount for transient simulations was obtained from equilibrium and spin-up periods directly for each grid cell in the region. To test the sensitivity to the initial soil carbon amount in transient simulations for the 21st century, we used empirical soil organic carbon data extracted from the Northern Circumpolar Soil Carbon Database (NCSCD)

240 (Tarnocai et al., 2009), as the initial soil carbon amount. The 0.5° × 0.5° soil carbon data
241 products for three different depths of 30cm, 100cm and 300cm were used. The sensitivity test
242 was conducted for transient simulations under the RCP 2.6 and RCP 8.5 scenarios. To avoid the
243 instability of C-N ratio caused by replacing the initial soil carbon pool with observed data at the
244 beginning of transient period, initial soil nitrogen values were also generated based on the soil
245 carbon data and corresponding C-N ratio map for transient simulations (Zhuang et al., 2003;
246 Raich and Schlesinger, 1992).

247

248 **3. Results**

249 **3.1 Model verification at site and regional levels**

250 With the optimized parameters, MIC-TEM reproduces the carbon dynamics well for alpine
251 tundra, boreal forest, temperate coniferous forest, temperate deciduous forest, grasslands and wet
252 tundra with R^2 ranging from 0.70 for Ivotuk to 0.94 for Bartlett Experimental Forest (Fig. S3,
253 table S3). In general, model performs better for forest ecosystems than for tundra ecosystems.
254 The temporal NPP from 2001 to 2010 simulated by MIC-TEM and TEM were compared with
255 MODIS NPP data (Fig. S4). Pearson correlation coefficients are 0.52 (MIC-TEM and MODIS)
256 and 0.34 (TEM and MODIS). NPP simulated by MIC-TEM showed higher spatial correlation
257 coefficients with MODIS data than TEM (Fig. S5). By considering more detailed microbial
258 activities, the heterotrophic respiration is more adequately simulated using the MIC-TEM. The
259 simulated differences in soil decomposition result in different levels of soil available nitrogen,
260 which influences the nitrogen uptake by plants, the rate of photosynthesis and NPP. The spatial

correlation coefficient between NPP simulated by MIC-TEM and MODIS is close to 1 in most study areas, suggesting the reliability of MIC-TEM at the regional scale.

3.2 Regional carbon dynamics during the 20th century

The equifinality of the parameters in MIC-TEM was considered in our ensemble regional simulations to measure the parameter uncertainty (Tang and Zhuang, 2008). Here and below, the ensemble means and the inter-simulation standard deviations are shown for uncertainty measure, unless specified as others. These ensemble simulations indicated that the northern high latitudes act from a carbon source of 38.9 PgC to a carbon sink of 190.8 PgC by different ensemble members, with the mean of 64.2±21.4 Pg at the end of 20th century while the simulation with the optimized parameters estimates a regional carbon sink of 77.6 Pg with the interannual standard deviation of 0.21 PgC yr^{-1} during the 20th century (Fig 1). Simulated regional NEP with optimized parameters using TEM and MIC-TEM showed an increasing trend throughout the 20th century except a slight decrease during the 1960s (Fig. 2). The Spatial distributions of NEP simulated by MIC-TEM for different periods in 20th century also show the increasing trend (Fig 3). Positive values of NEP represent sinks of CO_2 into terrestrial ecosystems, while negative values represent sources of CO_2 to the atmosphere. From 1900 onwards, both models estimated a regional carbon sink during the 20th century. With optimized parameters, TEM estimated higher NPP and R_H at 0.6 PgC yr^{-1} and 0.3 PgC yr^{-1} than MIC-TEM, respectively, at the end of the 20th century (Fig. 2). The MIC-TEM estimated a carbon sink increase from 0.64 to 0.83 PgCyr^{-1} during the century while the estimated increase by TEM was much higher (0.28 PgCyr^{-1}) (Fig. 2). At the end of the century, MIC-TEM estimated NEP reached 1.0 PgCyr^{-1} in comparison with

TEM estimates of 0.3 $PgCyr^{-1}$. TEM estimated NPP and R_H are 0.5 $PgCyr^{-1}$ and 0.3 $PgCyr^{-1}$ higher, respectively. As a result, TEM estimated that the region accumulated 11.4 Pg more carbon than MIC-TEM. Boreal forests are a major carbon sink at 0.55 and 0.63 $PgCyr^{-1}$ estimated by MIC-TEM and TEM, respectively. Alpine tundra contributes the least sink. Overall, TEM overestimated the sink by 12.5% in comparison to MIC-TEM for forest ecosystems and 16.7% for grasslands. For wet tundra and alpine tundra, TEM overestimated about 20% and 33% in comparison with MIC-TEM, respectively (Table 2).

3.3 Regional carbon dynamics during the 21st century

Regional annual NPP and R_H increases under the RCP 8.5 scenario according to simulations with both models (Fig. 4). With optimized parameters, MIC-TEM estimated NPP increases from 9.2 in the 2000s to 13.2 $PgCyr^{-1}$ in the 2090s, while TEM predicted NPP is 2.0 $PgCyr^{-1}$ higher in the 2000s and 0.3 $PgCyr^{-1}$ higher in the 2090s (Fig. 4). Similarly, TEM also overestimated R_H by 1.7 $PgCyr^{-1}$ in the 2000s and 0.25 $PgCyr^{-1}$ higher in the 2090s, respectively (Fig. 4). As a result, the regional sink increases from 0.53 $PgCyr^{-1}$ in the 2000s, 1.4 $PgCyr^{-1}$ in the 2070s, then decreases to 1.1 $PgCyr^{-1}$ in the 2090s estimated by MIC-TEM (Fig. 4). Given the uncertainty in parameters, MIC-TEM predicted the region acts as a carbon sink ranging from 48.7 to 140.7 Pg, with the mean of 71.7±26.6 Pg at the end of 21st century, while the simulation with optimized parameters estimates a regional carbon source of 79.5 Pg with the interannual standard deviation of 0.37 PgC yr^{-1} during the 21st century (Fig 4). TEM predicted a similar trend for NEP, which overestimated the carbon sink with magnitude of 19.2 Pg compared with the simulation by MIC-TEM with optimized parameters. Under the RCP 2.6 scenario (Fig. 4), the increase of NPP and

305 R_H is smaller from 2000 to 2100 compared to the simulation under the RCP 8.5. MIC-TEM
306 predicted that NPP increases from 9.1 to 10.9 PgCyr^{-1}, TEM estimated 1.6 PgCyr^{-1} higher at the
307 beginning and 0.9 PgCyr^{-1} higher in the end of the 21st century (Fig. 4). Consequently, MIC-
308 TEM predicted NEP fluctuates between sinks and sources during the century, with a neutral
309 before 2070, and a source between -0.2 - -0.3 Pg C yr^{-1} after the 2070s. As a result, the region
310 acts as a carbon source of 1.6 Pg C with the interannual standard deviation of 0.24 PgC yr^{-1}
311 estimated with MIC-TEM and a sink of 27.6 Pg C with the interannual standard deviation of 0.2
312 PgC yr^{-1} estimated with TEM during the century (Fig. 4). When considering the uncertainty
313 source of parameters, MIC-TEM predicted the region acts from a carbon source of 64.8 Pg C to a
314 carbon sink of 58.6 Pg C during the century with the mean of -3.3±20.3 Pg at the end of 21st
315 century (Fig 4).

316

317 **3.4 Model sensitivity to initial soil carbon**

318 Under the RCP 2.6, without replacing the initial soil carbon with inventory-based estimates[1] in
319 model simulations, TEM estimated that the regional soil organic carbon (SOC) is 604.2 Pg C and
320 accumulates 12.1 Pg C during the 21st century. When using estimated soil carbon[1] within depths
321 of 30cm, 100cm and 300cm as initial pools in simulations, TEM predicted that regional SOC is
322 429.5, 689.3 and 1003.4 Pg C in 2000, and increases by 9.9, 16.0 and 22.8 Pg C at the end of the
323 21st century, and the regional cumulative carbon sink is 20.4, 34.0, and 48.1 Pg C, respectively
324 during the century. In contrast, using the same inventory-based SOC estimates, MIC-TEM
325 projected that the region acts from a cumulative carbon sink to a source at 0.7, 2.2, and 3.0 Pg C,

respectively. Under the RCP 8.5, both models predicted that the region acts as a carbon sink, regardless of the magnitudes of initial soil carbon pools used, with TEM projected sink of 71.7, 120, and 155.6 Pg C and a much smaller cumulative sink of 65.4, 88.6, and 109.8 Pg C estimated with MIC-TEM, respectively (Table 3).

4. Discussion

During the last few decades, a greening accompanying warming and rising atmospheric CO_2 in the northern high latitudes (>45° N) has been documented (McGuire et al., 1995; McGuire and Hobbie, 1997; Chapin and Starfield, 1997; Stow et al., 2004; Callaghan et al., 2005; Tape et al., 2006). The large stocks of carbon contained in the region (Tarnocai et al., 2009) are particularly vulnerable to climate change (Schuur et al., 2008; McGuire et al., 2009). To date, the degree to which the ecosystems may serve as a source or a sink of C in the future are still uncertain (McGuire et al., 2009; Wieder et al., 2013). Therefore, accurate models are essential for predicting carbon–climate feedbacks in the future (Todd-Brown et al., 2013). Our regional simulations indicate the region is currently a carbon sink, which is consistent with many previous studies (White et al., 2000; Houghton et al., 2007), and this sink will grow under the RCP 8.5 scenario, but shift to a carbon source under the RCP 2.6 scenario by 2100. MIC-TEM shows a higher correlation between NPP and soil temperature (R=0.91) than TEM (R=0.82), suggesting that MIC-TEM is more sensitive to environmental changes (Table S4).

Our regional estimates of carbon fluxes by MIC-TEM are within the uncertainty range from other existing studies. For instance, Zhuang et al. (2003) estimated the region as a sink of 0.9 $PgCyr^{-1}$ in extratropical ecosystems for the 1990s, which is similar to our estimation of 0.83 $PgCyr^{-1}$ by MIC-TEM. White et al. (2000) estimated that, during the 1990s, regional NEP above

348 50 °N region is 0.46 $PgCyr^{-1}$ while Qian et al. (2010) estimated that NEP increased from 0 to 0.3
349 $PgCyr^{-1}$ for the high-latitude region above 60 °N during last century, and reached 0.25 $PgCyr^{-1}$
350 during the 1990s. White et al. (2000) predicted that, from 1850 to 2100, the region accumulated
351 134 PgC in terrestrial ecosystems, in comparison with our estimates of 77.6 PgC with MIC-TEM
352 and 89 PgC with TEM. Our projection of a weakening sink during the second half of the 21^{st}
353 century is consistent with previous model studies (Schaphoff et al., 2013). Our predicted trend of
354 NEP is very similar to the finding of White et al. (2000), indicating that NEP increases from 0.46
355 $PgCyr^{-1}$ in the 2000s and reaches 1.5 $PgCyr^{-1}$ in the 2070s, then decreases to 0.6 $PgCyr^{-1}$ in the
356 2090s.

357 The MIC-TEM simulated NEP generally agrees with the observations. However, model
358 simulations still deviate from the observed data, especially for tundra ecosystems. The deviation
359 may be due to the uncertainty or errors in the observed data, which do not well constrain the
360 model parameters. Uncertain driving data such as temperature and precipitation are also a source
361 of uncertainty for transient simulations. In addition, we assumed that vegetation will not change
362 during the transient simulation. However, over the past few decades in the northern high latitudes,
363 temperature increases have led to vegetation changes (Hansen et al., 2006), including latitudinal
364 treeline advance (Lloyd et al., 2005) and increasing shrub density (Sturm et al., 2001). Vegetation
365 can shift from one type to another because of competition for light, N and water (White et al.,
366 2000). For example, needleleaved trees tend to replace tundra gradually in response to warming.
367 In some areas, forests even moved several hundreds of kilometers within 100 years (Gear and
368 Huntley, 1991). The vegetation changes will affect carbon cycling in these ecosystems. In
369 addition, we have not yet considered the effects of management of agriculture lands (Cole et al.,

370 1997), but Zhuang et al. (2003) showed that the changes in agricultural land use in northern high
371 latitudes have been small.

372 The largest limitation to this study is that we have not explicitly considered the fire
373 effects. Warming in the northern high latitudes could favor fire in its frequency, intensity,
374 seasonality and extent (Kasischke and Turetsky, 2006; Johnstone and Kasischke, 2005; Soja et al.,
375 2007; Randerson et al., 2006; Bond-Lamberty et al., 2007). Fire has profound effects on northern
376 forest ecosystems, altering the N cycle and water and energy exchanges between the atmosphere
377 and ecosystems. Increase in wildfires will destroy most of above-ground biomass and consume
378 organic soils, resulting in less carbon uptake by vegetation (Harden et al., 2000), leading to a net
379 release of carbon in a short term. However, a suite of biophysical mechanisms of ecosystems
380 including post-fire increase in the surface albedo and rates of biomass accumulation may in turn,
381 exert a negative feedback to climate warming (Amiro et al., 2006; Goetz et al., 2007), further
382 influence the carbon exchanges between ecosystems and the atmosphere.

383 Moreover, carbon uptake in land ecosystems depends on new plant growth, which
384 connects tightly with the availability of nutrients such as mineral nitrogen. Recent studies have
385 shown that when soil nitrogen is in short supply, most terrestrial plants would form symbiosis
386 relationships with fungi; hyphae provides nitrogen to plants, in return, plants provide sugar to
387 fungi (Hobbie and Hobbie, 2008, 2006; Schimel and Hättenschwiler, 2007). This symbiosis
388 relationship has not been considered in our current modeling, which may lead to a large
389 uncertainty in our quantification of carbon and nitrogen dynamics.

Shift in microbial community structure was not considered in our model, which could affect the temperature sensitivity of heterotrophic respiration (Stone et al., 2012). Michaelis-Menten constant (K_m) could also adapt to climate warming, and it may increase more significantly with increasing temperature in cold-adapted enzymes than in warm-adapted enzymes (German et al., 2012; Somero et al., 2004; Dong and Somero, 2009). Carbon use efficiency (CUE) is also a controversial parameter in our model. Empirical studies in soils suggest that microbial CUE declines by at least 0.009 $^oC^{-1}$ (Steinweg et al., 2008), while other studies find that CUE is invariant with temperature (López-Urrutia and Morán, 2007). Another key microbial trait lacking in our modeling is microbial dormancy (He et al., 2015). Dormancy is a common, bet-hedging strategy used by microorganisms when environmental conditions limit their growth and reproduction (Lennon and Jones, 2011). Microorganisms in dormancy are not able to drive biogeochemical processes such as soil CO_2 production, and therefore, only active microorganisms should be involved in utilizing substrates in soils (Blagodatskaya and Kuzyakov, 2013). Many studies have indicated that soil respiration responses to environmental conditions are more closely associated with the active portion of microbial biomass than total microbial biomass (Hagerty et al., 2014; Schimel and Schaeffer, 2012; Steinweg et al., 2013). Thus, the ignorance of microbial dormancy could fail to distinguish microbes with different physiological states, introducing uncertainties to our carbon estimation.

5. Conclusions

This study used a more detailed microbial biogeochemistry model to investigate the carbon dynamics in the region for the past and this century. Regional simulations using MIC-TEM indicated that, over the 20th century, the region is a sink of 77.6 Pg. This sink could reach to 79.5

412 Pg under the RCP 8.5 scenario or shift to a carbon source of 1.6 Pg under the RCP 2.6 scenario
413 during 21st century. On the other hand, traditional TEM overestimated the carbon sink under the
414 RCP 8.5 scenario with magnitude of 19.2 Pg than MIC-TEM, and predicted this region acting as
415 carbon sink with magnitude of 27.6 Pg under the RCP 2.6 scenario during 21st century. Using
416 recent soil carbon stock data as initial soil carbon in model simulations, the region was estimated
417 to shift from a carbon sink to a source, with total carbon release at 0.7- 3 Pg by 2100 depending
418 on initial soil carbon pools at different soil depths under the RCP 2.6 scenario. In contrast, the
419 region acts as a carbon sink at 55.4 - 99.8 Pg C in the 21st century under RCP 8.5 scenario.
420 Without considering more detailed microbial processes, models estimated that the region acts as
421 a carbon sink under both scenarios. Under the RCP 2.6 scenario, the cumulative sink ranges
422 from 9.9 to 22.8 Pg C. Under the RCP 8.5 scenario, the cumulative sink is even larger at 71.7 -
423 155.6 Pg C. This study indicated that more detailed microbial physiology-based
424 biogeochemistry models estimate carbon dynamics very differently from using a relatively
425 simple microbial decomposition-based model. The comparison with satellite products or other
426 estimates for the 20th century suggests that the more detailed microbial decomposition shall be
427 considered to adequately quantify C dynamics in northern high latitudes.

428

429

430 **Acknowledgments**

431 This research was supported by a NSF project (IIS-1027955), a DOE project (DE-SC0008092),
432 and a NASA LCLUC project (NNX09AI26G) to Q. Z. We acknowledge the Rosen High

Performance Computing Center at Purdue for computing support. We thank the National Snow and Ice Data center for providing Global Monthly EASE-Grid Snow Water Equivalent data, National Oceanic and Atmospheric Administration for North American Regional Reanalysis (NARR), and Hugelius and his group by making available pan-Arctic permafrost soil C maps. We also acknowledge the World Climate Research Programme's Working Group on Coupled Modeling Intercomparison Project CMIP5, and we thank the climate modeling groups for producing and making available their model output. The data presented in this paper can be accessed through our research website (http://www.eaps.purdue.edu/ebdl/)

References

Allison, S. D., and Martiny, J. B.: Colloquium paper: resistance, resilience, and redundancy in microbial communities, Proceedings of the National Academy of Sciences of the United States of America, 105 Suppl 1, 11512-11519, 10.1073/pnas.0801925105, 2008.

Allison, S. D., Wallenstein, M. D., and Bradford, M. A.: Soil-carbon response to warming dependent on microbial physiology, Nature Geoscience, 3, 336-340, 10.1038/ngeo846, 2010.

Amiro, B. D., Orchansky, A. L., Barr, A. G., Black, T. A., Chambers, S. D., Chapin Iii, F. S., Goulden, M. L., Litvak, M., Liu, H. P., McCaughey, J. H., McMillan, A., and Randerson, J. T.: The effect of post-fire stand age on the boreal forest energy balance, Agricultural and Forest Meteorology, 140, 41-50, 10.1016/j.agrformet.2006.02.014, 2006.

Barichivich, J., Briffa, K. R., Myneni, R. B., Osborn, T. J., Melvin, T. M., Ciais, P., Piao, S., and Tucker, C.: Large-scale variations in the vegetation growing season and annual cycle of atmospheric CO2 at high northern latitudes from 1950 to 2011, Global change biology, 19, 3167-3183, 10.1111/gcb.12283, 2013.

Blagodatskaya, E., and Kuzyakov, Y.: Active microorganisms in soil: Critical review of estimation criteria and approaches, Soil Biology and Biochemistry, 67, 192-211, 10.1016/j.soilbio.2013.08.024, 2013.

Bond-Lamberty, B., Peckham, S. D., Ahl, D. E., and Gower, S. T.: Fire as the dominant driver of central Canadian boreal forest carbon balance, Nature, 450, 89-92, 10.1038/nature06272, 2007.

Bond-Lamberty, B., and Thomson, A.: Temperature-associated increases in the global soil respiration record, Nature, 464, 579-582, 10.1038/nature08930, 2010.

Callaghan, T., Björn, L. O., Chernov, Y., Chapin, T., Christensen, T. R., Huntley, B., Ims, R., Jolly, D., Jonasson, S., Matveyeva, N., Panikov, N., Oechel, W., and Shaver, G.: Arctic tundra and polar desert ecosystems, Arctic climate impact assessment, 243-352, 2005.

Chapin, F. S., and Starfield, A. M.: Time lags and novel ecosystems in response to transient climatic change in arctic Alaska, Climatic change, 35, 449-461, 1997.
Christensen, J. H., and Christensen, O. B.: A summary of the PRUDENCE model projections of changes in European climate by the end of this century, Climatic Change, 81, 7-30, 10.1007/s10584-006-9210-7, 2007.
Ciais, P., Sabine, C., Bala, G., Bopp, L., Brovkin, V., Canadell, J., Chhabra, A., DeFries, R., Galloway, J., Heimann, M., Jones, C., Quéré, C. L., Myneni, R. B., Piao, S., and Thornton, P.: Carbon and other biogeochemical cycles, Climate change 2013: the physical science basis. Contribution of Working Group I to the Fifth Assessment Report of the Intergovernmental Panel on Climate Change, 465-570, 2014.
Cole, C. V., Duxbury, J., Freney, J., Heinemeyer, O., K.Minami, Mosier, A., Paustian, K., Rosenberg, N., Sampson, N., Sauerbeck, D., and Zhao, Q.: Global estimates of potential mitigation of greenhouse gas emissions by agriculture, Nutrient cycling in Agroecosystems, 49, 221-228, 1997.
Davidson, E. A., Trumbore, S. E., and Amundson, R.: Biogeochemistry: soil warming and organic carbon content, Nature, 408, 2000.
Davidson, E. A., and Janssens, I. A.: Temperature sensitivity of soil carbon decomposition and feedbacks to climate change, Nature, 440, 165-173, 10.1038/nature04514, 2006.
Dong, Y., and Somero, G. N.: Temperature adaptation of cytosolic malate dehydrogenases of limpets (genus Lottia): differences in stability and function due to minor changes in sequence correlate with biogeographic and vertical distributions, The Journal of experimental biology, 212, 169-177, 10.1242/jeb.024505, 2009.
Duan, Q., Sorooshian, S., and Gupta, V. K.: Optimal use of the SCE-UA global optimization method for calibrating watershed models, Journal of Hydrology, 158, 265-284, 1994.
Esteban G. Jobbágy, and Jackson, R. B.: The vertical distribution of soil organic carbon and its relation to climate and vegetation, Ecological applications, 10, 423-436, 2000.
Gear, A. J., and Huntley, B.: Rapid changes in the range limits of Scots pine 4000 years ago, Science, 251, 544-547, 1991.
German, D. P., Marcelo, K. R. B., Stone, M. M., and Allison, S. D.: The Michaelis-Menten kinetics of soil extracellular enzymes in response to temperature: a cross-latitudinal study, Global change biology, 18, 1468-1479, 10.1111/j.1365-2486.2011.02615.x, 2012.
Goetz, S. J., Mack, M. C., Gurney, K. R., Randerson, J. T., and Houghton, R. A.: Ecosystem responses to recent climate change and fire disturbance at northern high latitudes: observations and model results contrasting northern Eurasia and North America, Environmental Research Letters, 2, 045031, 10.1088/1748-9326/2/4/045031, 2007.
Hagerty, S. B., van Groenigen, K. J., Allison, S. D., Hungate, B. A., Schwartz, E., Koch, G. W., Kolka, R. K., and Dijkstra, P.: Accelerated microbial turnover but constant growth efficiency with warming in soil, Nature Climate Change, 4, 903-906, 10.1038/nclimate2361, 2014.
Hansen, J., Sato, M., Ruedy, R., Lo, K., Lea, D. W., and Medina-Elizade, M.: Global temperature change, Proceedings of the National Academy of Sciences of the United States of America, 103, 14288-14293, 10.1073/pnas.0606291103, 2006.
Hanson, P. J., Edwards, N. T., Garten, C. T., and Andrews, J. A.: Separating root and soil microbial contributions to soil respiration: A review of methods and observations, Biogeochemistry, 48, 115-146, 2000.

Hao, G., Zhuang, Q., Zhu, Q., He, Y., Jin, Z., and Shen, W.: Quantifying microbial ecophysiological effects on the carbon fluxes of forest ecosystems over the conterminous United States, Climatic Change, 133, 695-708, 10.1007/s10584-015-1490-3, 2015.
Harden, J. W., Trumbore, S. E., Stocks, B. J., Hirsch, A., Gower, S. T., O'neill, K. P., and Kasischke, E. S.: The role of fire in the boreal carbon budget, Global change biology, 6, 174-184, 2000.
Harris, I., Jones, P. D., Osborn, T. J., and Lister, D. H.: Updated high-resolution grids of monthly climatic observations - the CRU TS3.10 Dataset, International Journal of Climatology, 34, 623-642, 10.1002/joc.3711, 2014.
Hayes, D. J., Kicklighter, D. W., McGuire, A. D., Chen, M., Zhuang, Q., Yuan, F., Melillo, J. M., and Wullschleger, S. D.: The impacts of recent permafrost thaw on land–atmosphere greenhouse gas exchange, Environmental Research Letters, 9, 045005, 10.1088/1748-9326/9/4/045005, 2014.
He, Y., Yang, J., Zhuang, Q., Harden, J. W., McGuire, A. D., Liu, Y., Wang, G., and Gu, L.: Incorporating microbial dormancy dynamics into soil decomposition models to improve quantification of soil carbon dynamics of northern temperate forests, Journal of Geophysical Research: Biogeosciences, 120, 2596-2611, 10.1002/2015jg003130, 2015.
Hobbie, E. A., and Hobbie, J. E.: Natural Abundance of 15N in Nitrogen-Limited Forests and Tundra Can Estimate Nitrogen Cycling Through Mycorrhizal Fungi: A Review, Ecosystems, 11, 815-830, 10.1007/s10021-008-9159-7, 2008.
Hobbie, J. E., and Hobbie, E. A.: 15N in symbiotic fungi and plants estimates nitrogen and carbon flux rates in Arctic tundra, Ecology, 87, 816-822, 2006.
Holland, M. M., and Bitz, C. M.: Polar amplification of climate change in coupled models, Climate Dynamics, 21, 221-232, 10.1007/s00382-003-0332-6, 2003.
Houghton, R. A.: Balancing the Global Carbon Budget, Annual Review of Earth and Planetary Sciences, 35, 313-347, 10.1146/annurev.earth.35.031306.140057, 2007.
Johnstone, J. F., and Kasischke, E. S.: Stand-level effects of soil burn severity on postfire regeneration in a recently burned black spruce forest, Canadian Journal of Forest Research, 35, 2151-2163, 10.1139/x05-087, 2005.
Kasischke, E. S., and Turetsky, M. R.: Recent changes in the fire regime across the North American boreal region—Spatial and temporal patterns of burning across Canada and Alaska, Geophysical Research Letters, 33, 10.1029/2006gl025677, 2006.
Knorr, W.: Annual and interannual CO2 exchanges of the terrestrial biosphere: process-based simulations and uncertainties, Global Ecology and Biogeography, 9, 225-252, 2000.
Lawrence, D. M., Oleson, K. W., Flanner, M. G., Thornton, P. E., Swenson, S. C., Lawrence, P. J., Zeng, X., Yang, Z.-L., Levis, S., Sakaguchi, K., Bonan, G. B., and Slater, A. G.: Parameterization improvements and functional and structural advances in Version 4 of the Community Land Model, Journal of Advances in Modeling Earth Systems, 3, 10.1029/2011ms000045, 2011.
Lennon, J. T., and Jones, S. E.: Microbial seed banks: the ecological and evolutionary implications of dormancy, Nature reviews. Microbiology, 9, 119-130, 10.1038/nrmicro2504, 2011.
Lloyd, A. H.: Ecological histories from Alaskan tree lines provide insight into future change, Ecology, 86, 1687-1695, 2005.

Mack, M. C., Schuur, E. A. G., Bret-Harte, M. S., Shaver, G. R., and III, F. S. C.: Ecosystem carbon storage in arctic tundra reduced by long-term nutrient fertilization, Nature, 431, 2004.
McGuire, A. D., Melillo, J. M., Joyce, L. A., Kicklighter, D. W., Grace, A. L., III, B. M., and Vorosmarty, C. J.: Interactions between carbon and nitrogen dynamics in estimating net primary productivity for potential vegetation in North America, Global Biogeochemical Cycles, 6, 101-124, 1992.
McGuire, A. D., Melillo, J. M., Kicklighter, D. W., and Joyce, L. A.: Equilibrium responses of soil carbon to climate change: Empirical and process-based estimates, Journal of Biogeography, 785-796, 1995.
McGuire, A. D., and Hobbie, J. E.: Global climate change and the equilibrium responses of carbon storage in arctic and subarctic regions, In Modeling the Arctic system: A workshop report on the state of modeling in the Arctic System Science program, 53-54, 1997.
McGuire, A. D., Anderson, L. G., Christensen, T. R., Dallimore, S., Guo, L., Hayes, D. J., Heimann, M., Lorenson, T. D., Macdonald, R. W., and Roulet, N.: Sensitivity of the carbon cycle in the Arctic to climate change, Ecological Monographs, 79, 523-555, 2009.
McGuire, A. D., Christensen, T. R., Hayes, D., Heroult, A., Euskirchen, E., Kimball, J. S., Koven, C., Lafleur, P., Miller, P. A., Oechel, W., Peylin, P., Williams, M., and Yi, Y.: An assessment of the carbon balance of Arctic tundra: comparisons among observations, process models, and atmospheric inversions, Biogeosciences, 9, 3185-3204, 10.5194/bg-9-3185-2012, 2012.
Melillo, J. M., McGuire, A. D., Kicklighter, D. W., III, B. M., Vorosmarty, C. J., and Schloss, A. L.: Global climate change and terrestrial net primary production, Nature, 363, 1993.
Oechel, W. C., Vourlitis, G. L., Hastings, S. J., Zulueta, R. C., Hinzman, L., and Kane, D.: Acclimation of ecosystem CO 2 exchange in the Alaskan Arctic in response to decadal climate warming, Nature, 406, 978, 2000.
Orchard, V. A., and Cook, F. J.: Relationship between soil respiration and soil moisture, 15, 447-453, 1983.
Parton, W. J., Ojima, D. S., Cole, C. V., and Schimel, D. S.: A general model for soil organic matter dynamics: sensitivity to litter chemistry, texture and management, Quantitative modeling of soil forming processes, 147-167, 1994.
Potter, C. S., Randerson, J. T., Field, C. B., Matson, P. A., Vitousek, P. M., Mooney, H. A., and Klooster, S. A.: Terrestrial ecosystem production: a process model based on global satellite and surface data, Global Biogeochemical Cycles, 7, 811-841, 1993.
Qian, H., Joseph, R., and Zeng, N.: Enhanced terrestrial carbon uptake in the Northern High Latitudes in the 21st century from the Coupled Carbon Cycle Climate Model Intercomparison Project model projections, Global change biology, 16, 641-656, 10.1111/j.1365-2486.2009.01989.x, 2010.
Raich, J. W., and Schlesinger, W. H.: The global carbon dioxide flux in soil respiration and its relationship to vegetation and climate, Tellus B, 44, 81-99, 1992.
Randerson, J. T., Liu, H., Flanner, M. G., Chambers, S. D., Jin, Y., Hess, P. G., Pfister, G., Mack, M. C., Treseder, K. K., Welp, L. R., Chapin, F. S., Harden, J. W., Goulden, M. L., Lyons, E., Neff, J. C., Schuur, E. A. G., and Zender, C. S.: The impact of boreal forest fire on climate warming, science, 1130-1132, 2006.

Running, S. W., and Coughlan, J. C.: A general model of forest ecosystem processes for regional applications I. Hydrologic balance, canopy gas exchange and primary production processes., Ecological Modelling, 42, 125-154, 1988.
Schaphoff, S., Heyder, U., Ostberg, S., Gerten, D., Heinke, J., and Lucht, W.: Contribution of permafrost soils to the global carbon budget, Environmental Research Letters, 8, 014026, 10.1088/1748-9326/8/1/014026, 2013.
Schimel, J.: The implications of exoenzyme activity on microbial carbon and nitrogen limitation in soil: a theoretical model, Soil Biology and Biochemistry, 35, 549-563, 10.1016/s0038-0717(03)00015-4, 2003.
Schimel, J.: Microbes and global carbon, Nature Climate Change, 3, 867-868, 10.1038/nclimate2015, 2013.
Schimel, J. P., and Hättenschwiler, S.: Nitrogen transfer between decomposing leaves of different N status, Soil Biology and Biochemistry, 39, 1428-1436, 10.1016/j.soilbio.2006.12.037, 2007.
Schimel, J. P., and Schaeffer, S. M.: Microbial control over carbon cycling in soil, Frontiers in microbiology, 3, 348, 10.3389/fmicb.2012.00348, 2012.
Schmidt, M. W., Torn, M. S., Abiven, S., Dittmar, T., Guggenberger, G., Janssens, I. A., Kleber, M., Kogel-Knabner, I., Lehmann, J., Manning, D. A., Nannipieri, P., Rasse, D. P., Weiner, S., and Trumbore, S. E.: Persistence of soil organic matter as an ecosystem property, Nature, 478, 49-56, 10.1038/nature10386, 2011.
Schuur, E. A. G., Bockheim, J., Canadell, J. G., Euskirchen, E., Field, C. B., Goryachkin, S. V., Hagemann, S., Kuhry, P., Lafleur, P. M., Lee, H., and Mazhitova, G.: Vulnerability of permafrost carbon to climate change: Implications for the global carbon cycle, BioScience, 58, 701-714, 2008.
Serreze, M. C., and Francis, J. A.: The Arctic on the fast track of change, Weather, 61, 65-69, 2006.
Soja, A. J., Tchebakova, N. M., French, N. H. F., Flannigan, M. D., Shugart, H. H., Stocks, B. J., Sukhinin, A. I., Parfenova, E. I., Chapin, F. S., and Stackhouse, P. W.: Climate-induced boreal forest change: Predictions versus current observations, Global and Planetary Change, 56, 274-296, 10.1016/j.gloplacha.2006.07.028, 2007.
Somero, G. N.: Adaptation of enzymes to temperature: searching for basic "strategies", Comparative biochemistry and physiology. Part B, Biochemistry & molecular biology, 139, 321-333, 10.1016/j.cbpc.2004.05.003, 2004.
Steinweg, J. M., Plante, A. F., Conant, R. T., Paul, E. A., and Tanaka, D. L.: Patterns of substrate utilization during long-term incubations at different temperatures, Soil Biology and Biochemistry, 40, 2722-2728, 10.1016/j.soilbio.2008.07.002, 2008.
Steinweg, J. M., Dukes, J. S., Paul, E. A., and Wallenstein, M. D.: Microbial responses to multi-factor climate change: effects on soil enzymes, Frontiers in microbiology, 4, 146, 10.3389/fmicb.2013.00146, 2013.
Stone, M. M., Weiss, M. S., Goodale, C. L., Adams, M. B., Fernandez, I. J., German, D. P., and Allison, S. D.: Temperature sensitivity of soil enzyme kinetics under N-fertilization in two temperate forests, Global change biology, 18, 1173-1184, 10.1111/j.1365-2486.2011.02545.x, 2012.

639 Stow, D. A., Hope, A., McGuire, D., Verbyla, D., Gamon, J., Huemmrich, F., Houston, S.,
640 Racine, C., Sturm, M., Tape, K., Hinzman, L., Yoshikawa, K., Tweedie, C., Noyle, B.,
641 Silapaswan, C., Douglas, D., Griffith, B., Jia, G., Epstein, H., Walker, D., Daeschner, S.,
642 Petersen, A., Zhou, L., and Myneni, R.: Remote sensing of vegetation and land-cover change in
643 Arctic Tundra Ecosystems, Remote Sensing of Environment, 89, 281-308,
644 10.1016/j.rse.2003.10.018, 2004.
645 Sturm, M., Racine, C., and Tape, K.: Climate change: increasing shrub abundance in the Arctic.,
646 Nature, 411, 2001.
647 Tang, J., and Zhuang, Q.: Equifinality in parameterization of process-based biogeochemistry
648 models: A significant uncertainty source to the estimation of regional carbon dynamics, Journal
649 of Geophysical Research: Biogeosciences, 113, 10.1029/2008jg000757, 2008.
650 Tape, K. E. N., Sturm, M., and Racine, C.: The evidence for shrub expansion in Northern Alaska
651 and the Pan-Arctic, Global change biology, 12, 686-702, 10.1111/j.1365-2486.2006.01128.x,
652 2006.
653 Tarnocai, C., Canadell, J. G., Schuur, E. A. G., Kuhry, P., Mazhitova, G., and Zimov, S.: Soil
654 organic carbon pools in the northern circumpolar permafrost region, Global Biogeochemical
655 Cycles, 23, n/a-n/a, 10.1029/2008gb003327, 2009.
656 Todd-Brown, K. E. O., Hopkins, F. M., Kivlin, S. N., Talbot, J. M., and Allison, S. D.: A
657 framework for representing microbial decomposition in coupled climate models,
658 Biogeochemistry, 109, 19-33, 10.1007/s10533-011-9635-6, 2011.
659 Todd-Brown, K. E. O., Randerson, J. T., Post, W. M., Hoffman, F. M., Tarnocai, C., Schuur, E.
660 A. G., and Allison, S. D.: Causes of variation in soil carbon simulations from CMIP5 Earth
661 system models and comparison with observations, Biogeosciences, 10, 1717-1736, 10.5194/bg-
662 10-1717-2013, 2013.
663 White, A., Cannell, M. G. R., and Friend, A. D.: The high-latitude terrestrial carbon sink: a
664 model analysis Global change biology, 6, 227-245, 2000.
665 Wieder, W. R., Bonan, G. B., and Allison, S. D.: Global soil carbon projections are improved by
666 modelling microbial processes, Nature Climate Change, 3, 909-912, 10.1038/nclimate1951, 2013.
667 Zhuang, Q., Romanovsky, V. E., and McGuire, A. D.: Incorporation of a permafrost model into a
668 large-scale ecosystem model: Evaluation of temporal and spatial scaling issues in simulating soil
669 thermal dynamics, Journal of Geophysical Research: Atmospheres, 106, 33649-33670,
670 10.1029/2001jd900151, 2001.
671 Zhuang, Q., McGuire, A. D., O'Neill, K. P., Harden, J. W., Romanovsky, V. E., and Yarie, J.:
672 Modeling soil thermal and carbon dynamics of a fire chronosequence in interior Alaska, Journal
673 of Geophysical Research, 108, 10.1029/2001jd001244, 2002.
674 Zhuang, Q., He, J., Lu, Y., Ji, L., Xiao, J., and Luo, T.: Carbon dynamics of terrestrial
675 ecosystems on the Tibetan Plateau during the 20th century: an analysis with a process-based
676 biogeochemical model, Global Ecology and Biogeography, no-no, 10.1111/j.1466-
677 8238.2010.00559.x, 2010.
678 Zhuang, Q., Chen, M., Xu, K., Tang, J., Saikawa, E., Lu, Y., Melillo, J. M., Prinn, R. G., and
679 McGuire, A. D.: Response of global soil consumption of atmospheric methane to changes in
680 atmospheric climate and nitrogen deposition, Global Biogeochemical Cycles, 27, 650-663,
681 10.1002/gbc.20057, 2013.

Zhuang, Q., Zhu, X., He, Y., Prigent, C., Melillo, J. M., David McGuire, A., Prinn, R. G., and Kicklighter, D. W.: Influence of changes in wetland inundation extent on net fluxes of carbon dioxide and methane in northern high latitudes from 1993 to 2004, Environmental Research Letters, 10, 095009, 10.1088/1748-9326/10/9/095009, 2015.
Zhuang, Q., McGuire, A. D., Melillo, J. M., Clein, J. S., Dargaville, R. J., Kicklighter, D. W., Myneni, R. B., Dong, J., Romanovsky, V. E., Harden, J., and Hobbie, J. E.: Carbon cycling in extratropical terrestrial ecosystems of the Northern Hemisphere during the 20th century: a modeling analysis of the influences of soil thermal dynamics, Tellus B: Chemical and Physical Meteorology, 55, 751-776, 10.3402/tellusb.v55i3.16368, 2003.
Zimov, S. A., Schuur, E. A. G., and III, F. S. C.: Permafrost and the global carbon budget, Science, 312, 1612-1613, 2006.

Author contributions. Q.Z. designed the study. J.Z. conducted model development, simulation and analysis. J.Z. and Q. Z. wrote the paper.

Competing financial interests. The submission has no competing financial interests.

Materials & Correspondence. Correspondence and material requests should be addressed to qzhuang@purdue.edu.

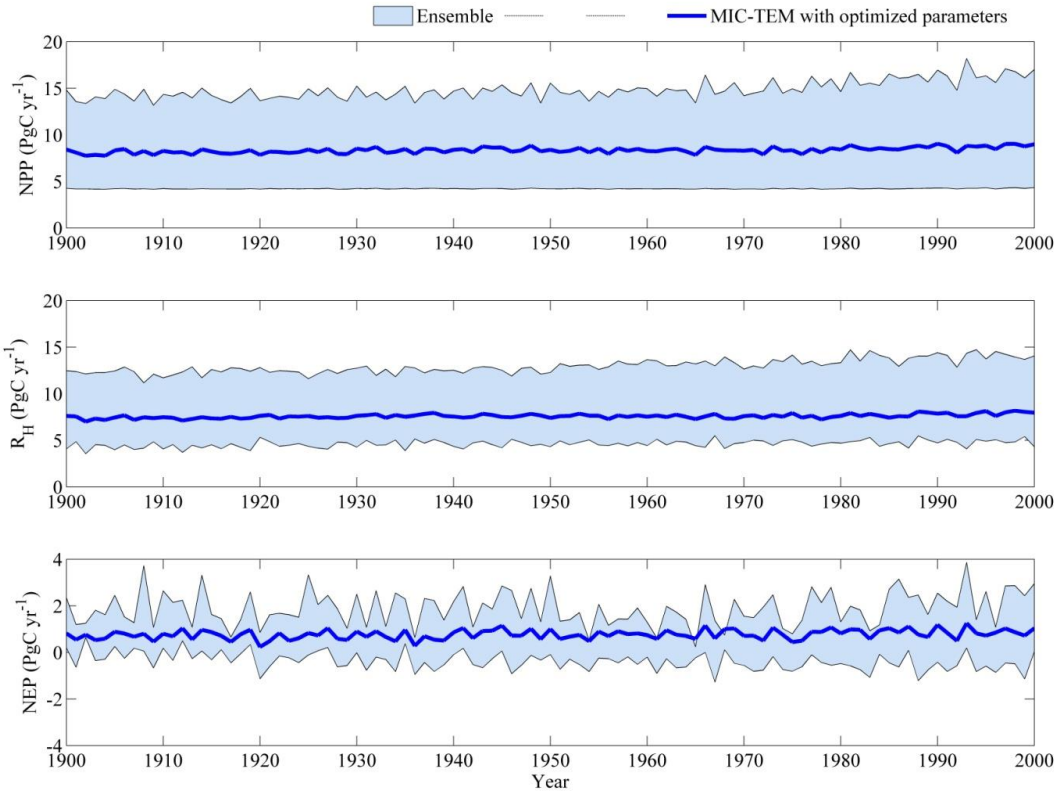

Figure 1. Simulated annual net primary production (NPP, top panel), heterotrophic respiration (R_H, center panel) and net ecosystem production (NEP, bottom panel) by MIC-TEM with ensemble of parameters.

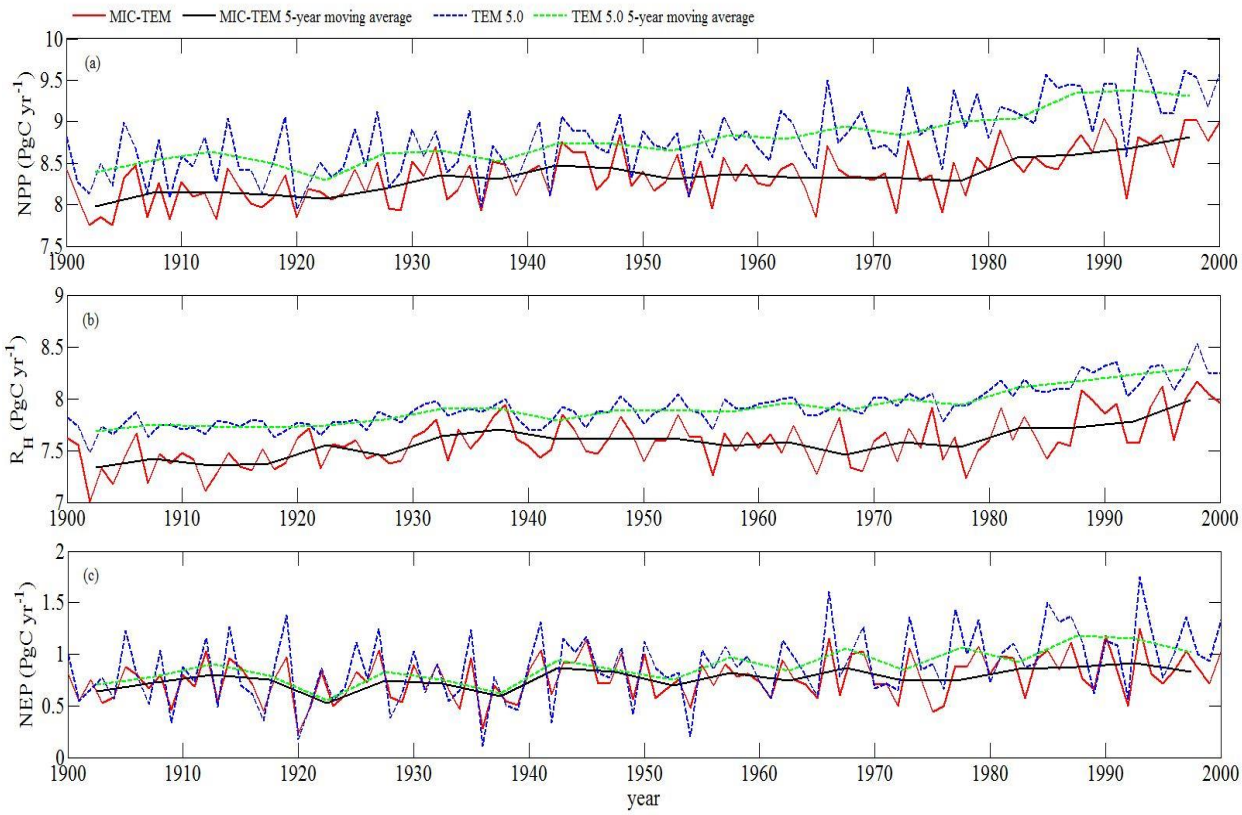

Figure 2. Simulated annual net primary production (NPP, top panel), heterotrophic respiration (R_H, center panel) and net ecosystem production (NEP, bottom panel) by MIC-TEM and TEM, respectively.

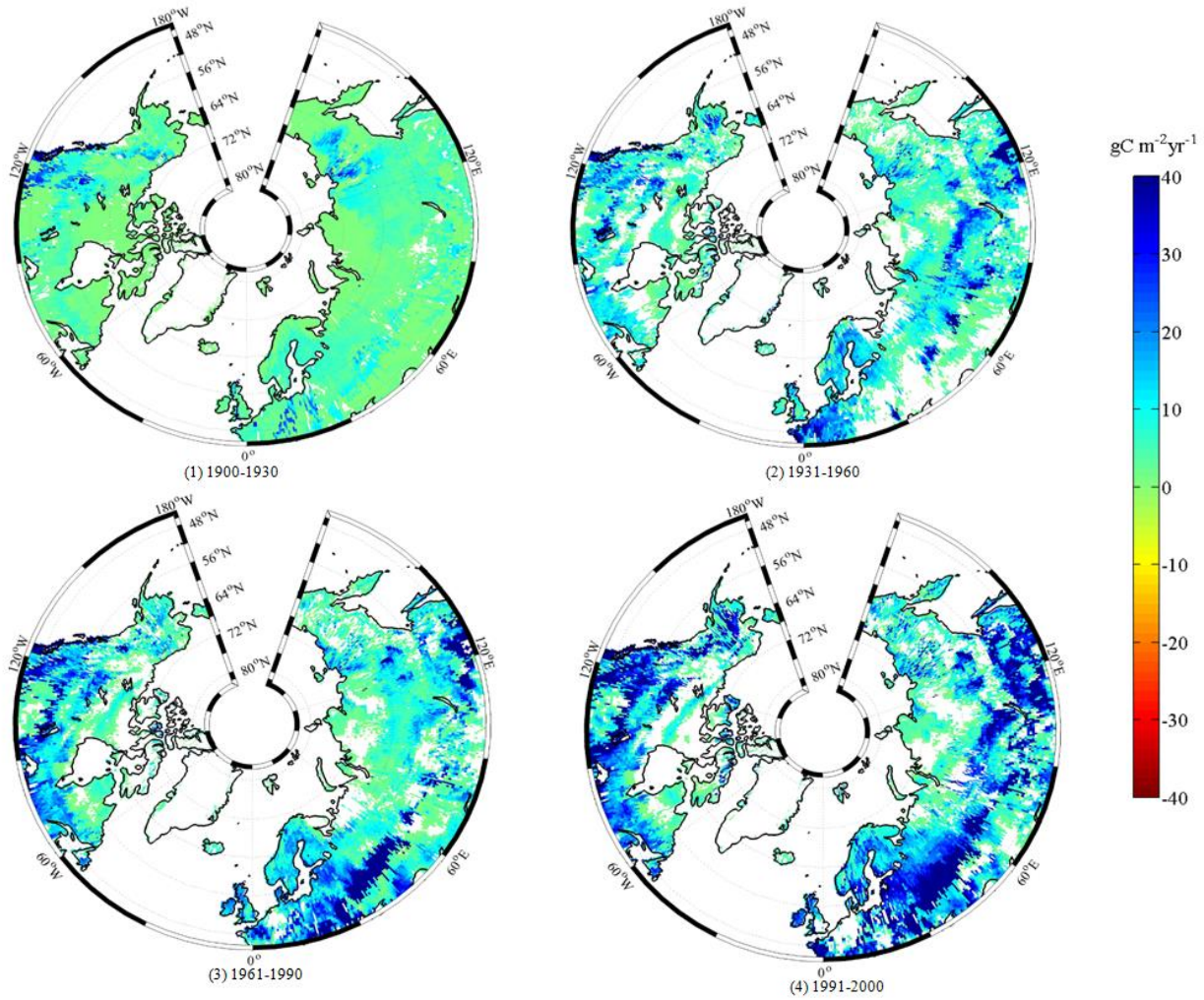

Figure 3. Spatial distribution of NEP simulated by MIC-TEM for the periods: (1) 1900-1930, (2) 1931-1960, (3) 1961-1990, and (4) 1991-2000. Positive values of NEP represent sinks of CO_2 into terrestrial ecosystems, while negative values represent sources of CO_2 to the atmosphere.

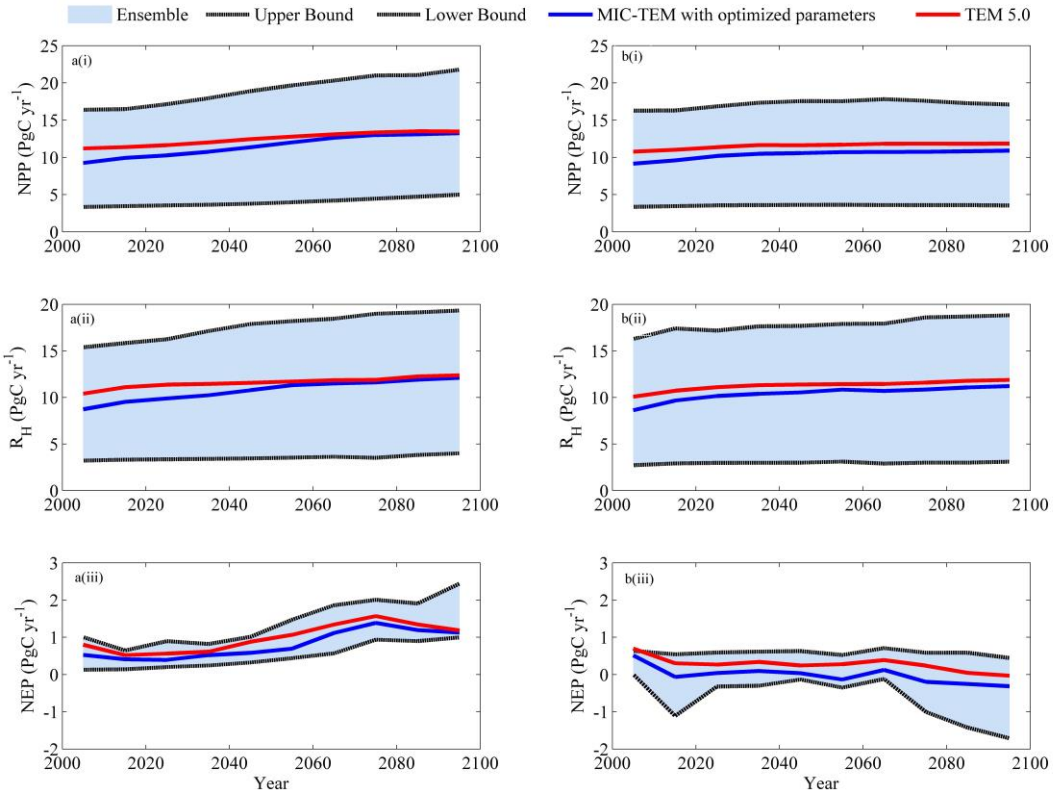

Figure 4. Predicted changes in carbon fluxes: (i) NPP, (ii) R_H, and (iii) NEP for all land areas north of 45 °N in response to transient climate change under (a) RCP 8.5 scenario and (b) RCP 2.6 scenario with MIC-TEM and TEM 5.0, respectively. The decadal running mean is applied. The grey area represents the upper and lower bounds of simulations.

Table 1. Parameters associated with more detailed microbial dynamics in MIC-TEM

Process	Parameter	Units	Initial Value	Description	Parameter range	Reference
Assimilation	$Vmax_{uptake_0}$	mg DOC cm^{-3} (mg biomass cm^{-3})$^{-1}$ h^{-1}	9.97e6	Maximum microbial uptake rate	[1.0e4, 1.0e8]	Hao et al. (2015)
	Ea_{uptake}	kJ mol^{-1}	47	Activation energy	-	Allison et al. (2010)
	$Km_{uptake_{slope}}$	mg cm^{-3} $degree^{-1}$	0.01	Temperature regulator of MM for DOC uptake by microbes	-	Allison et al. (2010)
	Km_{uptake_0}	mg cm^{-3}	0.1	Temperature regulator of MM for DOC uptake by microbes	-	Allison et al. (2010)
CO_2 production	CUE_{slope}	$degree^{-1}$	-0.016	Temperature regulator of carbon use efficiency	-	Allison et al. (2010)
	CUE_0	-	0.63	Temperature regulator of carbon use efficiency	-	Allison et al. (2010)
Decay	$Vmax_0$	mg SOC cm^{-3} (mg Enz cm^{-3})$^{-1}$ h^{-1}	9.17e7	Maximum rate of converting SOC to soluble C	[1.0e5, 1.0e8]	Hao et al. (2015)
	Ea	kJ mol^{-1}	47	Activation energy	-	Allison et al. (2010)
	Km_{slope}	mg cm^{-3} $degree^{-1}$	5	Temperature regulator of MM for enzymatic decay	-	Allison et al. (2010)
	Km_0	mg cm^{-3}	500	Temperature regulator of MM for enzymatic decay	-	Allison et al. (2010)
MIC turnover	r_{death}	s^{-1}	0.02	Microbial death fraction	-	Allison et al. (2010)
	MICtoSOC		50	Partition coefficient for dead microbial biomass between the SOC and DOC pool	-	Allison et al. (2010)
ENZ turnover	$r_{EnzProd}$	s^{-1}	5.0e-4	Enzyme production fraction	-	Allison et al. (2010)
	$r_{EnzLoss}$	s^{-1}	0.1	Enzyme loss fraction	-	Allison et al. (2010)

Table 2. Partitioning of average annual net ecosystem production (as Pg C per year) for six vegetation types during the 20th century

	MIC-TEM (PgC yr^{-1})	TEM 5.0 (PgC y^{-1})
Alpine tundra	0.03	0.04
Boreal forest	0.39	0.45
Conifer forest	0.09	0.09
Deciduous forest	0.16	0.18
Grassland	0.06	0.07
Wet tundra	0.05	0.06
Total	0.78	0.89

Table 3. Increasing of SOC, vegetation carbon (VGC), soil organic nitrogen (SON), vegetation nitrogen (VGN) from 1900 to 2000, and total carbon storage during the 21st century predicted by two models with observed soil carbon data of three different depths under (a) RCP 2.6 and (b) RCP 8.5.

(a)

Model	Units: Pg	Without (control)	30cm	100cm	300cm
TEM 5.0	SOC/SON in 2000	604.2/27.0	429.5/19.0	689.3/31.6	1003.4/46.2
	Increase of SOC during the 21st century	12.1	9.9	16.0	22.8
	VGC/VGN in 2000	318.3/1.48	238.4/1.05	394.2/1.80	556.7/2.53
	Increase of VGC during the 21st century	15.5	10.5	18.0	25.3
	Increase of total carbon storage during the 21st century	27.6	20.4	34.0	48.1
MIC-TEM	SOC/SON in 2000	591.5/26.8	420.3/18.6	686.0/31.2	990.7/45.3
	Increase of SOC during the 21st century	-2.0	-1.2	-2.4	-2.9
	VGC/VGN in 2000	309.7/1.42	230.1/1.02	374.4/1.71	548.6/2.45
	Increase of VGC during the 21st century	0.4	0.5	0.2	-0.1
	Increase of total carbon storage during the 21st century	-1.6	-0.7	-2.2	-3.0

(b)

Model	Units: Pg	Without (control)	30cm	100cm	300cm
TEM 5.0	SOC/SON in 2000	610.2 /27.9	431.9/19.1	693.8/31.8	1007.1/46.4
	Increase of SOC during the 21st century	44.2	33.0	56.5	74.6
	VGC/VGN in 2000	324.9/1.50	242.1/1.07	399.6/1.83	570.2/2.57
	Increase of VGC during the 21st century	54.5	38.7	63.5	81.0
	Increase of total carbon storage during the 21st century	98.7	71.7	120.0	155.6
MIC-TEM	SOC/SON in 2000	596.0/27.1	424.6/18.8	689.1/31.5	995.5/46.1
	Increase of SOC during the 21st century	33.3	27.4	36.9	42.9
	VGC/VGN in 2000	316.0/1.44	233.5/1.02	380.0/1.72	568.3/2.56
	Increase of VGC during the 21st century	46.2	37.0	51.7	56.9
	Increase of total carbon storage during the 21st century	79.5	65.4	88.6	109.8